state, an ultrafast routing controller (TOAD1 with $\Delta x = \tau \cdot c/2$) that all-optically sets the state of the routing switch (TOAD2), and an optical buffer that matches the delay of the input packet to the processing delay of the routing controller. Fig. 2*a* shows the input multiplexed high intensity clock and two packets: '1110..0' and '1010..0'. The 4ps temporal separation of the header bits results in the different headers appearing as cumulative 'double height' (101 bit sequence) and 'triple height' (111 bit sequence) pulses when observed on a limited bandwidth oscilloscope (Fig. 2*b*).

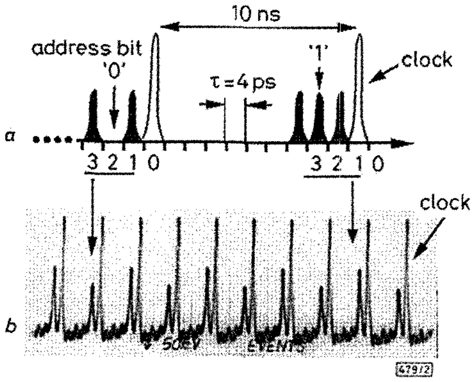

Fig. 2 *Node input*

a Timing diagram
b Incoming packets on limited bandwidth oscilloscope

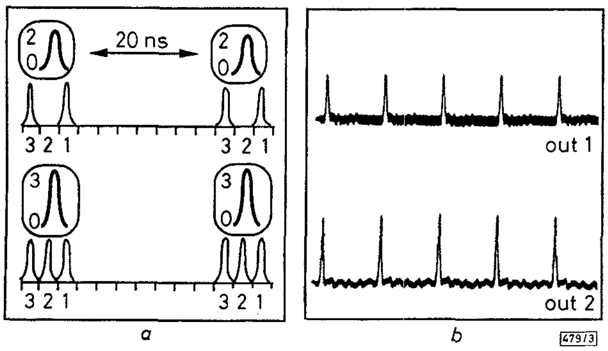

Fig. 3 *Output of switch: address bit '2' used as routing signal*

a Timing diagram (different packets appear as cumulative 'double height' (101 bit sequence) and 'triple height' (111 bit sequence) pulses on a limited bandwidth oscilloscope)
b Experimental demonstration

After entering the node, the clock is separated from the optical packet using a polarisation beam splitter, PS. Before entering the buffer, a portion (10%) of the packet is split off and sent to TOAD1 which then reads the packet destination address bit. The demultiplexed address bit, after passing through an optical isolator (OI), is amplified in a semiconductor optical amplifier (SOA) and then used as the optical routing control for the routing switch (TOAD2).

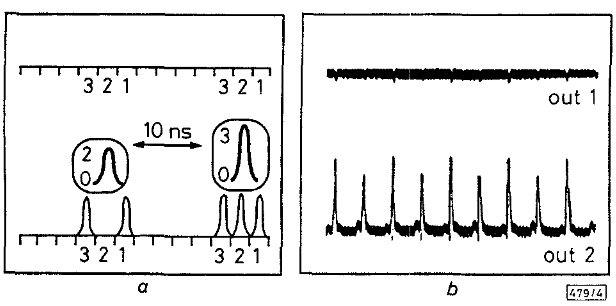

Fig. 4 *Output of switch: address bit '1' used as routing signal*

a Timing diagram (different packets appear as cumulative 'double height' (101 bit sequence) and 'triple height' (111 bit sequence) pulses on limited bandwidth oscilloscope
b Experimental demonstration

In a single bit routing scheme, we first use address bit 2 (alternately '1' or '0') as the routing bit for TOAD2. Packets with address bit 2 of value '1' are routed to output port out 2, while packets with an address bit of value '0' are routed to output port out 1. This results in triple height pulses (the packets with header '111') at output port out 2, and double height pulses (the packets with header '101') at output port out 1 (Fig. 3*a*). Fig. 3*b* is an oscilloscope photograph of the outputs of the routing switch TOAD2 as seen on a bandwidth limited oscilloscope. In the next experiment, we use bit 1 (always '1') as the routing bit. In this case, both packets are routed to output port out 2 (Fig. 4*a*). This results in zeros at output port out 1 and alternate double height (packets with header '101') and triple height (packets with header '111') pulses at output port out 2. Fig. 4*b* is an oscilloscope photograph of the outputs of routing switch TOAD2 as seen on a bandwidth limited oscilloscope.

In conclusion, we report the first demonstration of all-optical ultrafast switching with single bit all optical routing control in a banyan-type network. Both ultrafast address recognition and ultrafast routing of photonic packets were performed all-optically on a header in which the bit period was of only 4ps duration (e.g. at 250Gbit/s data rate). Photonic packets were self-routed through an all-optical ultrafast switch without the need for optoelectronic conversion. Two TOADs were used in different regimes: (i) as an ultrafast all-optical routing controller, and (ii) as an ultrafast all-optically controlled routing switch. The bit error rate at the switching element was measured to be $< 10^{-9}$. All of these results indicate that the TOAD is a well-suited device for applications in ultrafast all-optical banyan networks.

28 February 1997
Electronics Letters Online No: 19970494

I. Glesk, K.I. Kang and P.R. Prucnal (*Department of Electrical Engineering, Princeton University, Princeton, NJ 08544, USA*)

References

1 GLESK, I., SOKOLOFF, J.P., and PRUCNAL, P.R.: 'All-optical address recognition and self-routing in a 250Gb/s packet-switched network', *Electron. Lett.*, 1994, **30**, pp. 1322–1323

2 COTTER, D., LUCEK, J.K., SHABEER, M., SMITH, K., ROGERS, D.C., NESSET, D., and GUNNING, P.: 'Self-routing of 100Gbit/s packets using 6-bit 'keyword' address recognition', *Electron. Lett.*, 1995, **31**, pp. 1475–1476

3 GLESK, I., KANG, K.I., and PRUCNAL, P.R.: 'Ultrafast all-optically controlled 2×2 crossbar switch'. IEEE/LEOS '96 Annual Meeting, Boston, MA, 18–21 November 1996, Vol. 2, Paper WS3, p. 149

4 ADAMS, M.J., DAVIES, D.A.O., TATHAM, M.C., and FISHER, M.A.: 'Nonlinearities in semiconductor laser amplifiers', *Opt. Quantum Electron.*, 1995, **27**, (1), pp. 1–13

5 THYLÉN, L., KARISSON, G., and NILSSON, O.: 'Switching technologies for future guided wave optical networks: Potentials and limitations of photonics and electronics', *IEEE Commun. Mag.*, 1996, **34**, pp. 106–113

6 BLUMENTHAL, D.J.: 'Physics and applications of semiconductor optical amplifiers'. LEOS'96, 9th Annual Meeting, Boston, MA, USA, 18–21 November 1996

7 PRUCNAL, P.R.: 'Optically processed self-routing, synchronization, and contention resolution for 1-D and 2-D photonic switching architectures', *IEEE J. Quantum Electron.*, 1993, **29**, pp. 600–612

In-service passive surveillance system for optically-amplified branched networks

C.K. Chan, F. Tong, L.K. Chen and D. Lam

Indexing terms: Optical communication, Fault diagnosis

The authors experimentally demonstrate a passive surveillance system for in-service fault identification in optically-amplified branched networks. The proposed scheme only requires fibre Bragg gratings to be placed on different fibre branches and needs no extra laser source as required in conventional and multi-wavelength OTDR. The reflected monitoring channels are demultiplexed by an array-waveguide grating and detected by a power sensor array. The link status of all fibre branches can be monitored continuously and simultaneously through the Internet.

Introduction: Optically-amplified passive branched optical networks (OA-PBONs) are very promising and cost-effective architectures for future subscriber networks such as CATV and fibre-to-the-home systems. To ensure a reliable transmission of data channels over the subscriber networks and to maximise the link utilisation, it is essential to have a non-intrusive and cost-effective surveillance system to identify the faults along the fibre link in a timely manner and continuously while the data channels are still in service [1, 2]. Previously, we have proposed a passive surveillance scheme [3] for in-service fault identification using fibre Bragg gratings (FBGs) and the unused portions of the optical amplifier spectra as the sources. In this Letter, a system demonstration on this surveillance scheme is reported.

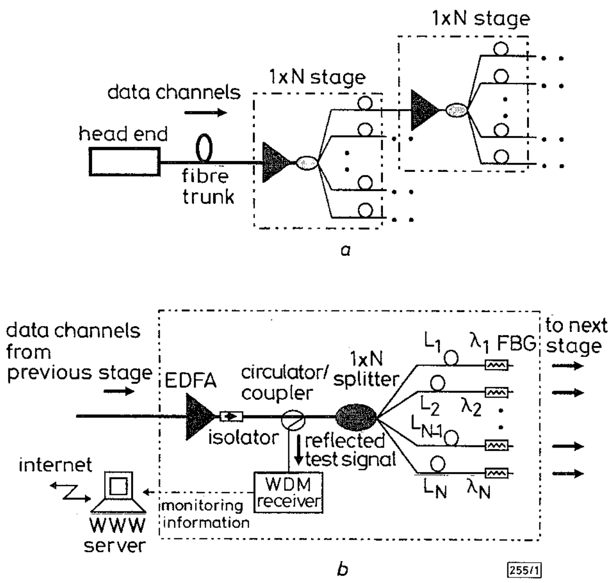

Fig. 1 *M-ary tree-branched OA-PBON and proposed in-service surveillance system for 1×N stage*

a M-ary tree-branched OA-PBON
b In-service surveillance system for 1×*N* stage
Note: optical isolator can be removed when optical circulator is used instead of coupler

Surveillance scheme: Fig. 1*a* shows the overall *M*-ary OA-PBON considered which consists of multiple 1×*N* stages. In each stage, an optical amplifier is placed before the *N*-splitting branches to compensate for the splitting and fibre attenuation losses (Fig. 1*b*). In our scheme, the unused spectra of the optical amplifier are used as the source, and no extra light sources are used as in conventional and multi-wavelength OTDR techniques [1, 2]. An FBG is placed on each branch to slice and reflect the amplifier's amplified spontaneous emission (ASE) power at a designated wavelength other than the data signal wavelengths and to form a monitoring channel for that branch. If an erbium-doped fibre amplifier (EDFA) is chosen as the amplifier, the wavelength ranges of the monitoring channels should be assigned at 1525–1540nm and 1556–1566nm, which are outside the EDFA's flat gain region reserved for carrying data signal wavelengths. The centre wavelengths for the FBGs in the N-branches are all different in the same stage, but identical wavelength assignment can be repeated in each stage since the positioning of the stage can simply be identified by the monitoring receiver responsible for that stage. The mass duplication of components reduces the manufacturing and maintenance costs and makes the entire surveillance scheme cost-effective. The monitoring signals are extracted using an optical circulator or a fibre coupler, and are detected by a WDM receiver in that stage. The WDM receiver can be an array-waveguide grating (AWG) followed by a power sensor array. Fault indications are judged by whether the reflected monitoring signals are above or below a certain decision threshold set by the comparator circuitry following the WDM receiver. Any abrupt link discontinuity between the FBG and the splitter is signified by a weak reflection in the monitoring channel, indicating that the branch is at fault. A healthy link condition is characterised by a strong reflection from the FBG. The monitoring information can be processed by simple circuitry following the WDM receiver before being transmitted back to the network operators.

Successful operation of the proposed scheme requires accommodation of the temperature changes which will detune the reflection centre wavelength of the FBGs in the branches. We assume that the WDM receiver operates in a thermally controlled environment. Such thermal detuning implies an increase in the spacing between the monitoring wavelengths, and thus limits the number of branches that can be monitored in each stage. Each passband of the WDM demultiplexer, measured at the crossover point, should at least cover the maximum spectral deviations derived from the temperature changes in the FBG. This is justifiable because for best performance, the decision threshold for the monitoring signals is set slightly above the noise level, a level well below the crossover point. Using an unused EDFA's ASE spectra of 23nm, thermal detuning of 0.01nm/°C in our typical FBG of bandwidth 1nm, and an operational temperature range of –4 to +44°C, the passband of the demultiplexer should be at least 1.48nm; the maximum number of available monitoring channels is ~15.

The setting for the decision threshold depends on the system configurations such as the amplifier gain, the number of optical channels, the distance separating the FBG from the power sensor, and the location of the fault along the fibre branch (near-far effect in back-scattering), etc. Disregarding the causes of the fault, the reflected monitoring signals mostly consist of unguided modes and should be very weak. The decision threshold can then be safely set at a few decibels above the maximum backreflection level when the fault occurs nearest to the WDM receiver.

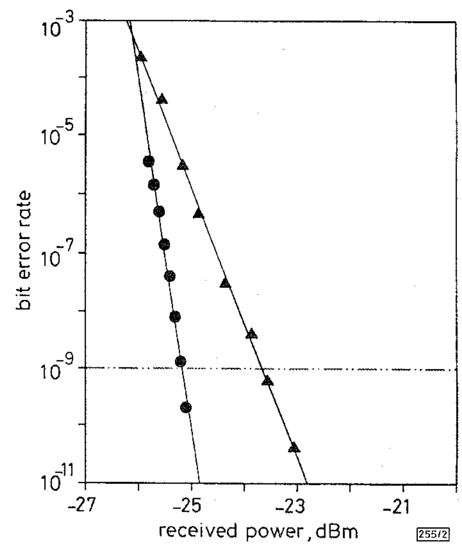

Fig. 2 *BER performance of 1Gbit/s (2^{10}–1 PRBS) NRZ data channel at 1555nm*

Detected at branch 1 with and without surveillance scheme:
● with scheme
▲ without scheme

Surveillance system: We demonstrate here a single 1×*N* stage system instead of an *M*-stage OA-PBON, since the *M*-stage is a mere duplication of multiple 1×*N* stages. The experimental setup is similar to that in Fig. 1*b*. The reflected monitoring channels are demultiplexed by an AWG (PIRI AWG-16×16-100G-1.5-1) and the outputs are connected to power sensors capable of detecting signal levels down to –90dBm. The monitored signals are continuously processed and the link status is automatically updated to a world-wide-web server which can be accessed by a remote site via the Internet.

In our demonstration, the 1×*N* stage has four branches (via a 1×4 coupler) with fibre lengths L_1 = 8.8km, L_2 = 6.6km, and FBG wavelengths centred at λ_1 = 1557.5nm, λ_2 = 1559.9nm; branches 3 and 4 are left unmonitored. The 3dB full-width passband, the thermal detuning and the reflectivity of each FBG (JDS FBG) used are 0.9nm, 0.01nm/°C and 90% respectively. The AWG used in the WDM receiver has an insertion loss of 4dB, a full-width 3dB passband of 0.4nm, a crosstalk level of –30dB and a crossover level of 17dB between adjacent passbands. A 1Gbit/s (2^{10}–1 PRBS) NRZ data channel at 1555nm with a transmitted power of 6dBm is inputted to the optical amplifier. Fig. 2 shows the bit error rate performance of the data channel at the end of branch 1; results without the surveillance scheme are also shown for reference. A Fabry-Perot optical filter with a 1nm 3dB full-width passband is used to reduce the ASE noise from the amplifier. As shown in the Figure, our scheme shows no observable degradation. Instead, there is ~1.3dB improvement in receiver sensitivity at $BER = 10^{-9}$ which is due to a reduction in the ASE noise power by the in-line FBG.

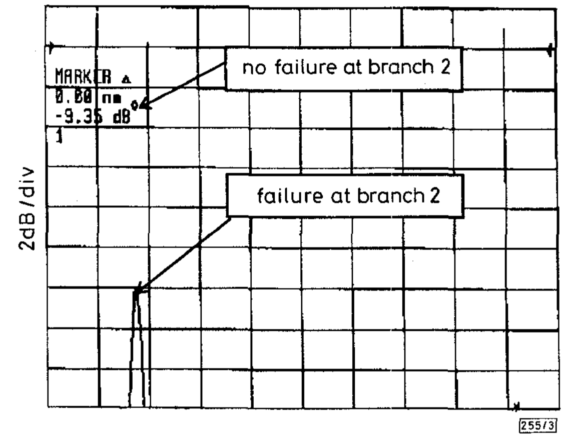

Fig. 3 *Output spectrum of AWG when branch 2 is disconnected*
Start 1556.26nm, stop 1574.07nm

To simulate the fault identification process, the fibre of branch 2 is intentionally disconnected at a location close to the FBG, and the reflected spectrum after the AWG is shown in Fig. 3. The decision threshold is set at –57dBm, taking into account the near-far effect of 2dB in backscattering. The measured peak reflection power at λ_2 at the WDM receiver before and after the disconnection are –50.5 and –61dBm, respectively, clearly indicating that branch 2 is at fault after the disconnection. Similar results are obtained for branch 1.

Summary: We have experimentally demonstrated the system operation of our proposed passive surveillance scheme for optically-amplified branched optical networks. The in-service data channels are not interrupted or degraded and the link status of all fibre branches can be monitored continuously and simultaneously by remote hosts via the Internet.

11 February 1997
Electronics Letters Online No: 19970509

C.K. Chan, F. Tong and L.K. Chen (*Department of Information Engineering, The Chinese University of Hong Kong, Shatin, NT, Hong Kong*)

D. Lam (*JDS FITEL Inc., Nepean, Ontario, K2G 5W8, Canada*)

F. Tong: On leave from IBM T.J. Watson Research Center, Yorktown Heights, NY, USA

E-mail: ckchan3@ie.cuhk.edu.hk

References

1 SANKAWA, I.: 'Fault location technique for in-service branched optical fibre networks', *IEEE Photonics Technol. Lett.*, 1990, **2**, (10), pp. 766–768

2 KOYAMADA, Y.: 'Recent progress in OTDR technologies for maintaining optical fibre networks'. IOOC'95, Hong Kong, 1995, Paper FA1-4

3 CHAN, C.K., TONG, F.K., CHEN, L.K., SONG, J., and LAM, K.W.: 'A practical passive surveillance scheme for optically-amplified passive branched optical networks', *IEEE Photonics Technol. Lett.*, 1997

Polarisation modulators with polygonal fibres

K. Yoshida, S. Nishikawa, T. Hikami, T. Sugimura, T. Yagi and T. Morikawa

Indexing terms: Optical modulation, Optical fibres

Polarisation modulators with either square fibres or regular octagonal fibres have been fabricated for the first time. The frequency responses of the modulators were measured and compared to a polarisation modulator with a round fibre. The results showed that the new modulators have a much higher modulation efficiency and a greater number of active frequency ranges than do round-fibre modulators.

External modulators are widely used both in optical sensors and for optical communications. If communication signals are converted to optical signals and transmitted through optical fibre from its side by using a modulator, it is possible to send various kinds of information, such as digital data and video signals, from multiple points through only one optical fibre. For phase modulation, various modulators have been fabricated [1 – 3]. However, the use of phase modulators in the transmission of video signals has not been reported because they do not have suitable frequency characteristics. In the case of polarisation modulators, Fujisaki *et al.* [4] realised a PZT modulator for an optical talk set, and the authors proposed a polarisation modulator which consists of a support substrate having a thin ZnO deposited layer and a round optical fibre [5, 6]. While two of that modulator in series make it independent of the polarisation of guided light, an AM video signal was sent through an optical fibre at an SNR of > 42dB [6].

However, this modulator has low sensitivity leading to difficulties in practical use. We therefore tried to improve the sensitivity of the modulator and realised new polarisation modulators. This report deseribes the improved modulators and their characteristics.

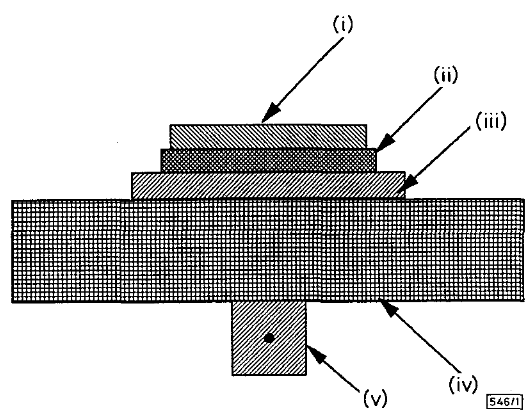

Fig. 1 *Configuration of fabricated polarisation modulator with square fibre*
(i) upper electrode, (ii) piezoelectric layer, (iii) lower electrode, (iv) support substrate, (v) square fibre

Fig. 1 shows a configuration of a fabricated polarisation modulator with a square fibre. This modulator has a square fibre instead of the round fibre in previous modulators [5, 6]. The new modulator consists of a support substrate which has a lower electrode, a thin piezoelectric film and an upper electrode which are sequentially deposited on the substrate, and a square fibre. The support substrate is a silica-glass plate of 0.3mm in thickness. The lower and upper electrodes are made from thin Au film deposited by a vacuum deposition technique. The piezoelectric film consists of a 5μm thick ZnO layer deposited by a magnetron sputtering machine. The polarisation modulator in Fig. 1 uses a regular octagonal fibre instead of a square fibre.

A square fibre and a regular octagonal fibre were fabricated by the method mentioned in [7]. Their core and cladding are made of GeO_2–SiO_2 and SiO_2 glass, respectively, and a relative refractive index difference of the core-cladding is 0.34%. The square fibre has 124.4μm long sides and a cutoff wavelength of 1.25μm. The attenuation loss is 0.69dB/km at 1.3μm and 0.80dB/km at 1.55μm.